Laboratori Nazionali di Frascati

LNF-68/77

M. Greco, A. Tenore and A. Verganelakis : VIRTUAL-PROTON COMPTON EFFECT AND THE ELECTRON (MUON)-PROTON BREMSSTRAHLUNG AS A TEST OF QUANTUM ELECTRODYNAMICS.

Estratto da : Nuovo Cimento 58A, 743 (1968)

M. GRECO, *et al.*
21 Dicembre 1968
Il Nuovo Cimento
Serie X, Vol. 58 A, pag. 743-767

Virtual-Proton Compton Effect and the Electron (Muon)-Proton Bremsstrahlung as a Test of Quantum Electrodynamics.

M. GRECO and A. TENORE

Laboratori Nazionali del CNEN - Frascati

A. VERGANELAKIS (*)

Istituto di Fisica dell'Università - Roma
Laboratori Nazionali del CNEN - Frascati

(ricevuto il 13 Luglio 1968)

Summary. — The virtual-proton Compton effect is studied in the approximation of a single virtual proton and a 3-3 resonance. The computation of the latter intermediate state is carried out in the framework of isobaric formalism. The contribution to the measurements of the wide-angle bremsstrahlung, arising from the virtual-proton Compton terms, is given explicitly. It is shown that these contributions depend strongly on the kinematical configuration of the experiments and may change appreciably the results of pure QED in the critical region where the intermediate electron or muon is far off its mass shell. The numerical results suggest that the exponential form factor is a more reasonable one, to describe the behaviour of the $\gamma\mathcal{N}\mathcal{N}^*$ vertex form factor. In addition it is pointed out that proton-polarization measurements in the wide-angle bremsstrahlung and large-angle pair-production experiments, provide one with a new important source of information about the contribution of the virtual-proton Compton effect to these processes. Polarized cross-sections are explicitly calculated.

1. – Introduction.

As is well known there are two complementary classes of experiments for studying the limts of validity of QED. These are the low-energy, high-accuracy

(*) On leave form NRC «Democritos», Athens.

atomic measurements (hydrogen hyperfine structure; Lamb shift, etc.) and high-energy, lower-accuracy measurements, large-angle pair production, wide-angle bremsstrahlung, etc.). The former class has been well studied in the past, while only recently, with the improvement of the experimental techniques, the latter has begun to be explored.

In fact in the last five years several high-energy experiments have been performed [1] or are now under way, which are designed to study the behaviour of amplitudes, in which an intermediate electron or muon is far off the mass shell.

Often the theoretical interpretation of these experiments goes as follows. First it is supposed that contributions to the measurements that are not interesting from the standpoint of testing QED, are known exactly. Secondly one calculates the amplitude of the QED process in conventional perturbation theory. Then one compares the ratio of the experimetal results to theoretical predictions, seeing to what extent various conjectured changes in the Green's function, in particular the electron (muon) propagator [2], are limited, or possibly required, by experiment.

In the case of the electron (muon)-proton wide-angle bremsstrahlung (WAB)

$$e(\mu) + p \to e(\mu) + p + \gamma\,, \tag{1.1}$$

the first-order Feynman diagrams are shown in Fig. 1: *a*) and *b*) are the so-called Bethe-Heitler (BH) diagrams and *c*) is the virtual-proton Compton (VPC) diagram. The contribution to the measurements arising from diagram *c*) is

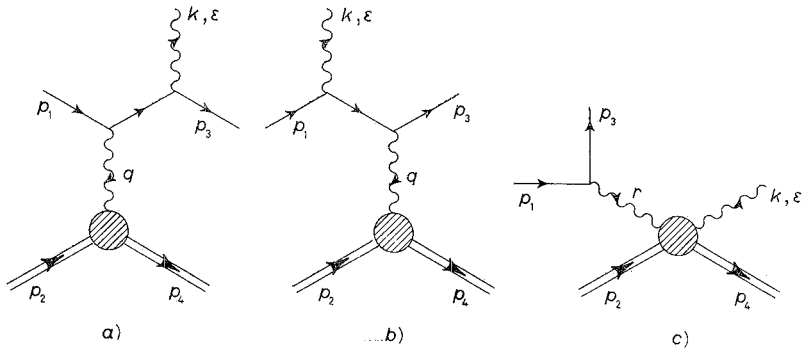

Fig. 1. – First-order Feynman diagrams for wide-angle bremsstrahlung: *a*), *b*) electron bremsstrahlung; *c*) proton bremsstrahlung.

---

[1] See *A review of recent work in experimental quantum electrodynamics*, by R. WEINSTEIN, *1967 International Symposium on Electron and Proton Interactions at High Energies*, (Stanford, Cal., 1967); D. QUINN and D. RITSON: *Phys. Rev. Lett.*, **20**, 890 (1968).

[2] J. A. MCCLURE and S. D. DRELL: *Nuovo Cimento*, **37**, 1638 (1965).

the uninteresting one for testing QED. However, it is desirable to know exactly this contribution, in order to avoid as far as possible the introduction of uncertainties into the interpretation of the experimental data. In principle the interference of diagram *c*) with the BH terms can be eliminated by using as probe particles both e^+ and e^- (μ^+ and μ^-) under exactly symmetrical kinematical configurations (*), but what always remains is the modulus of the amplitude of this diagram.

So far only the contributions arising from the single-nucleon intermediate state of the diagram 1 *c*) have been evaluated [4]. Previous attempts to estimate the contribution of the $N^*(1238)$ resonance intermediate state suffered from many poorly justified approximations [5].

We have tried to improve the accuracy to which the contribution of the VPC amplitude to the WAB is known, by approximating the blob of the diagram of Fig. 1 *c*) by the contributions of a single virtual proton and a 3-3 resonance. The computation of the latter intermediate-state contribution has been carried out in the framework of isobaric formalism, under the assumption that the 3-3 resonance is an elementary particle described by a Rarita-Schwinger spin-$\frac{3}{2}$ field. In a previous paper [6] we have reported explicit results showing that the importance of the VPC contribution to the WAB depends on the kinematical configuration of the experiment, and may change appreciably the results expected from pure QED, at critical points at which the intermediate electron or muon is far off its mass shell. Also we have suggested that the study of polarization phenomena in the WAB and large-angle pair-production experiments, provides us with a new source of information and helps us to gain a better understanding of the VPC effects, offering a test of the reliability of our calculations.

In view of the fact that in designing future experiments concerning the process (1), either for testing QED or for studing the VPC effect, more information will be needed, we report here an extensive description of the VPC amplitude as well as of various measurable quantities related to the WAB process. Direct application of the results given below is found also in the π^0-electroproduction experiments, in various sum rules, etc. On the other hand by making

---

(*) An analogous situation is found in the photoproduction of large-angle pairs in which the interference between the BH and VPC amplitude can be avoided in a symmetrical arrangement, where charges and polarizations of the final leptons are not observed [3].

[3] J. BJORKEN, S. DRELL and S. FRAUTSCHI: *Phys. Rev.*, **112**, 1409 (1958).

[4] R. A. BERG and C. N. LINDNER: *Phys. Rev.*, **112**, 2072 (1958); P. S. ISAEV and I. S. ZLATEV: *Nucl. Phys.*, **16**, 608 (1960); A. COSTESCU and T. VESCAN: *Nuovo Cimento*, **48**, 1041 (1967).

[5] R. A. BERG and C. N. LINDNER: *Nucl. Phys.*, **26**, 259 (1961).

[6] M. GRECO, A. TENORE and A. VERGANELAKIS: *Phys. Lett.* **27 B**, 317 (1968).

use of the substitution rule it is easy to extend these results to the photoproduction of large-angle pairs.

The program of the present paper is as follows. In Sect. **2** the form of the matrix element of the WAB process is given. Section **3** deals with the differential cross-section, unpolarized target; differential cross-section, polarized target; and polarization of the recoil proton. In Sect. **4** the VPC amplitude in the approximation of a single nucleon and 3-3 resonance intermediate state is given explicitly. In Sect. **5** our numerical calculations and results are reported and in Sect. **6** a discussion of our results is presented. In the Appendix we give the notation used and useful formulae.

2. – Form of the matrix element.

We begin by starting our notational conventions. We adopt the Lorentz signature $(+, -, -, -)$ for $g^{\mu\nu}$, the alternating tensor $\varepsilon_{\mu\nu\varrho\sigma}$ with $\varepsilon_{0123} = -\varepsilon^{0123} = +1$ and the four-vector p with components $p^\mu = (E, \boldsymbol{p})$, $\mu = 0, 1, 2, 3$. We use the notation $\tilde{p} = p^\mu \gamma_\mu$. For Dirac matrices and spinor normalization we use the same conventions as BJORKEN and DRELL (7).

Let us adopt the particle labels indicated in Fig. 1 where ε is the polarization four-vector of the real photon. The amplitude F is defined by

$$S = 1 + i(2\pi)^4 \delta^4(p_1 + p_2 - p_3 - p_4 - k) \left(\frac{m^2}{E_1 E_3}\right)^{\frac{1}{2}} \left(\frac{M^2}{E_2 E_4}\right)^{\frac{1}{2}} \left(\frac{1}{2k_0}\right)^{\frac{1}{2}} F \,. \tag{2.1}$$

We are using natural units ($\hbar = c = 1$). F may be written as the sum of two amplitudes:

$$F = F^{\mathrm{BH}} + F^{\mathrm{VPC}} \,, \tag{2.2}$$

where in F^{BH} and F^{VPC} are included the amplitudes of BH diagrams and of VPC diagrams respectively.

In conventional perturbation theory the F^{BH} has the form

$$F^{\mathrm{BH}} = c_1 \, \bar{u}(p_3) \varepsilon'^{\varrho} \, M'_{\varrho\lambda} \varepsilon^{\lambda} u(p_1) \,, \tag{2.3}$$

where ε is the real-photon polarization, c_1 is a constant, and

$$\varepsilon'_\varrho = \frac{1}{q^2} \bar{u}(p_4) \, \Gamma_\varrho u(p_2) \,, \tag{2.4}$$

$$\Gamma^\varrho = e \left\{ F_1(q^2) \gamma^\varrho + \frac{i\mu}{2M} F_2(q^2) \sigma^{\varrho\nu} q_\nu \right\} , \tag{2.5}$$

(7) J. BJORKEN and S. DRELL: *Relativistic Quantum Mechanics* (New York, 1964).

with $F_1(q^2)$ and $F_2(q^2)$ the Dirac and Pauli proton form factors respectively, normalized to $F_1(0)=F_2(0)=1$, μ is the anomalous magnetic moment in units of the nuclear magneton, and finally

$$M'_{\varrho\lambda}=\left(\frac{p_{3\lambda}}{p_3\cdot k}-\frac{p_{1\lambda}}{p_1\cdot k}\right)\gamma_\varrho+\left(\frac{\gamma_\varrho \tilde{k}\gamma_\lambda}{2p_1 k}+\frac{\gamma_\lambda \tilde{k}\gamma_\varrho}{2p_3\cdot k}\right) \tag{2.6}$$

is the matrix element of the virtual-electron Compton amplitude.

Similarly the F^{VPC} may be written

$$F^{\text{VPC}}=c_2\,\bar{u}(p_4)\,\varepsilon''_\mu M_{\mu\nu}\varepsilon^\nu u(p_2)\,, \tag{2.7}$$

where now the index ν refers to the real photon,

$$\varepsilon''_\mu=\frac{1}{r^2}\bar{u}(p_2)\gamma_\mu u(p_1) \tag{2.8}$$

and $M_{\mu\nu}$ denotes the virtual-proton Compton amplitude. Now pure QED cannot describe entirely the amplitude $M_{\mu\nu}$. However requiring Lorentz, parity and charge-conjugation invariance $M_{\mu\nu}$ can be written ([5]) in terms of twelve manifestly gauge-invariant amplitudes f_i $(i=1,\ldots,12)$. By keeping the same notation as in ref. ([5]), one has in our conventions

$$\begin{aligned}M_{\mu\nu}=&\frac{C_\mu C_\nu}{MC^2}\left[f_1+\frac{1}{M}\tilde{K}f_2\right]+\frac{D_\mu D_\nu}{MD^2}\left[f_3+\frac{1}{M}\tilde{K}f_4\right]+\\&+\frac{M(C_\mu D_\nu+D_\mu C_\nu)}{D^2}\left[i\gamma_5 f_5+\frac{1}{M^3}\tilde{D}f_6\right]+\frac{M(C_\mu D_\nu-C_\mu D_\nu)}{D^2}\left[i\gamma_5 f_7+\frac{1}{M^3}\tilde{D}f_8\right]+\\&+\frac{MA'_\mu C_\nu}{A^2C^2}\left[f_9+\frac{1}{M}\tilde{K}f_{10}\right]+\frac{M^3A'_\mu D_\nu}{A^2D^2}\left[i\gamma_5 f_{11}+\frac{1}{M^3}\tilde{D}f_{12}\right],\end{aligned} \tag{2.9}$$

where A_μ, B_μ, C_μ and D_μ are four orthogonal four-vectors, chosen as basic vectors, defined as follows:

$$\begin{aligned}&A_\mu=K_\mu=\tfrac{1}{2}(r+k)_\mu\,, \qquad Q_\mu=\tfrac{1}{2}(r-k)_\mu\,, \qquad R_\mu=\tfrac{1}{2}(p_2+p_4)_\mu,\\&B_\mu=Q_\mu-\frac{Q\cdot K}{K^2}K_\mu, \qquad C_\mu=R_\mu-\frac{R\cdot K}{K^2}K_\mu-\frac{R\cdot B}{B^2}B_\mu\,,\\&D_\mu=\varepsilon_{\mu\alpha\beta\gamma}A^\alpha B^\beta C^\gamma\end{aligned}$$

and $A'_\mu=A_\mu+xB_\mu$ with x defined in the Appendix. As been shown in ref. ([5])

the twelve amplitudes f_i are functions of three invariants choosen to be the ν_1, ν_2 and ν_3 defined in the Appendix. In the case that both photons are real the twelve f_i are reduced to the following six f_j ($j = 1, 2, 3, 4, 6, 7$).

3. – Wide-angle bremsstrahlung cross-sections.

The differential cross-section for the process (1.1), in terms of the matrix element F defined in (2.1) is given by

$$(3.1)\quad \mathrm{d}\sigma = \frac{1}{(2\pi)^5}\frac{m^2M^2}{2\sqrt{(p_1\cdot p_2)^2 - m^2M^2}}|F|^2\delta^4(p_1+p_2-p_3-p_4-k)\frac{\mathrm{d}^3p_3}{E_3}\frac{\mathrm{d}^3p_4}{E_4}\frac{\mathrm{d}^3k}{k_0},$$

where, due to eq. (2.2)

$$(3.2)\qquad |F|^2 = |F^{\mathrm{BH}}|^2 + |F^{\mathrm{VPC}}|^2 + 2\,\mathrm{Re}\,(F^{\mathrm{BH}})^*\cdot F^{\mathrm{VPC}}.$$

We give the explicit expression of (3.1) in the following particular cases.

3·1. *Differential cross-section, unpolarized target.* – If the polarizations are not observed, we must average over initial, and sum over final, spins.

Then eq. (3.1) becomes

$$(3.3)\quad \mathrm{d}\sigma = \frac{M^2\alpha^3}{2\pi^2\sqrt{(p_1\cdot p_2)^2 - m^2M^2}}\cdot \{I_1+I_2+I_3\}\delta^4(p_1+p_2-p_3-p_4-k)\frac{\mathrm{d}^3p_3}{E_3}\frac{\mathrm{d}^3p_4}{E_4}\frac{\mathrm{d}^3k}{k_0},$$

where $\alpha = e^2/4\pi$, and I_1, I_2 and I_3 are given by

$$(3.4)\quad I_1 = \frac{1}{q^4}\left\{\mathscr{F}_1(q^2)\left[-\frac{\lambda_1}{\lambda_2}-\frac{\lambda_2}{\lambda_1}-\frac{m^2q^2}{2\lambda_1^2}-\frac{m^2q^2}{2\lambda_2^2}-\frac{r^2q^2}{2\lambda_1\lambda_2}\right]+\mathscr{F}_2(q^2)\cdot\right.$$
$$\cdot\left[-\frac{m^2}{2M^2}\left(\frac{\mu_1+\mu_4}{\lambda_2}-\frac{\mu_2+\mu_3}{\lambda_1}\right)^2-\frac{q^2}{4M^2}\left(\frac{(\mu_1+\mu_4)^2+(\mu_2+\mu_3)^2}{\lambda_1\lambda_2}\right)+\frac{m^2q^2}{\lambda_1\lambda_2}\left(1-\frac{q^2}{4M^2}\right)\right]+$$
$$\left.+\mathscr{F}_3(q^2)\left[\left(\frac{m^2}{\lambda_1}-\frac{m^2}{\lambda_2}\right)-\frac{1}{2}\left(\frac{m^2}{\lambda_1}-\frac{m^2}{\lambda_2}\right)^2\right]\right\},$$

with

$$(3.5a)\qquad \mathscr{F}_1(q^2) \equiv F_1^2+\frac{1}{4}(F_1^2+4F_1F_2\mu+F_2^2\mu^2)\frac{q^2}{M^2}+\frac{\mu^2F_2^2}{16}\left(\frac{q^2}{M^2}\right)^2,$$

$$(3.5a)\qquad \mathscr{F}_2(q^2) \equiv F_1^2-\frac{\mu^2q^2}{4M^2}F_2^2, \qquad \mathscr{F}_3(q^2) \equiv (F_1+\mu F_2)^2\frac{q^2}{M^2};$$

$$(3.6)\qquad I_2 = -\frac{4}{q^2 r^2}\frac{1}{4\nu_4^2-\nu_2^2}\cdot$$
$$\cdot\left[(f_1, f_2)y_1 + (f_3, f_4)y_2 + (f_9, f_{10})y_3 + (F_1+\mu F_2)\frac{q^2}{M^2}\sum_{n=1}^{6} Z_n \operatorname{Re}(f_{2n})\right],$$

with

$$(3.7)\qquad (f_i, f_j) \equiv F_1(q^2)\operatorname{Re}(f_i + \nu_1 f_j) + \frac{\mu q^2}{4M^2}F_2(q^2)\operatorname{Re}(f_i);$$

$$(3.8)\quad I_3 = -\frac{2}{r^4}\left[\frac{4\nu_3^2\alpha_3}{\nu_2^4}(4\nu_4^2-\nu_2^2)J_1 + (\nu_3+\alpha_1^2\alpha_3)J_2 + (\nu_3+\alpha_2)J_3 - (8\nu_3\nu_4\alpha_1\alpha_3/\nu_2^2)J_4\right],$$

with

$$(3.9)\quad \begin{cases} J_1 \equiv [9, 10, 11, 12] \equiv |f_9+\nu_1 f_{10}|^2 + (\nu_2+\nu_3)\{|f_{12}|^2 - |f_9|^2 - \nu_2^{-2}|f_{11}|^2\} + \\ \qquad + \dfrac{\nu_1^2(\nu_2+\nu_3)^2}{\nu_2^2}|f_{12}|^2 - \nu_2^2\left\{|f_{10}|^2 + \left(\dfrac{\nu_2+\nu_3}{\nu_2}\right)^2|f_{12}|^2\right\}, \\ J_2 = [1, 2, 5+7, 6+8], \qquad J_3 = [3, 4, 5-7, 6-8], \\ J_4 = \operatorname{Re}\Big\{(f_1+\nu_1 f_2)(f_9^*+\nu_1 f_{10}^*) + (\nu_2+\nu_3)\cdot \\ \qquad \cdot[f_{12}^*(f_6+f_8) - f_1 f_9^* - \nu_2^{-2} f_{11}^*(f_5+f_7)] + \\ \qquad + \dfrac{\nu_1^2(\nu_2+\nu_3)^2}{\nu_2^2}(f_6+f_8)f_{12}^* - \nu_2^2\left[f_2 f_{10}^* + \left(\dfrac{\nu_2+\nu_3}{\nu_2}\right)^2(f_6+f_8)f_{12}^*\right]\Big\}. \end{cases}$$

In other words I_1 is the BH term, I_2 the interference between BH and VPC amplitudes and I_3 is the VPC term. The notation used is given in the Appendix and it is the same as that of BERG and LINDER [5] to make easier the comparison of the formulae. The above results are in agreement with those obtained previously by these authors.

In coincidence experiments, in which the quantity

$$\left.\frac{\mathrm{d}^5\sigma}{\mathrm{d}\Omega_3\mathrm{d}\Omega_4\mathrm{d}E_4}\right|_{\mathrm{lab}}$$

is measured, eq. (3.3) becomes

$$(3.10)\qquad \left.\frac{\mathrm{d}^5\sigma}{\mathrm{d}\Omega_3\mathrm{d}\Omega_4\mathrm{d}E_4}\right|_{\mathrm{lab}} = \frac{\alpha^3}{2\pi^2}\frac{M}{k_0}\frac{\boldsymbol{p}_3^2}{E_3}\frac{|\boldsymbol{p}_4|}{|\boldsymbol{p}_1|}\frac{1}{(|\boldsymbol{p}_3|/E_3) - \hat{p}_3\cdot\hat{k}}\{I_1+I_2+I_3\}.$$

In the case that only one final particle is observed this formula has to be integrated properly.

3·2. *Differential cross-section, polarized target.* – We describe the two possible spin states of a fermion of momentum p by the covariant projection operators (7)

$$P(\pm s) = \tfrac{1}{2}(1 \pm \gamma_5 \tilde{s}) , \tag{3.11}$$

where s is the spin of the proton

$$s \cdot p = 0 , \qquad s^2 = -1 .$$

We consider a WAB process in which the initial proton (target) is polarized long s, and we define the quantity

$$R = \frac{\mathrm{d}\sigma(+s) - \mathrm{d}\sigma(-s)}{\mathrm{d}\sigma(+s) + \mathrm{d}\sigma(-s)} , \tag{3.12}$$

where $\mathrm{d}\sigma(\pm s)$ is the differential cross-section of WAB with the two possible spin states. With this definition we find that R is written

$$R = \frac{\dfrac{M^2\alpha^3}{2\pi^2\sqrt{(p_1\cdot p_2)^2 - m^2M^2}} \{II_2 + II_3\}\, \delta^4(p_1 + p_2 - p_3 - p_4 - k) \dfrac{\mathrm{d}^3p_3}{E_3} \dfrac{\mathrm{d}^3p_4}{E_4} \dfrac{\mathrm{d}^3k}{k_0}}{\mathrm{d}\sigma_{\mathrm{unpol}}} , \tag{3.13}$$

where II_2 and II_3 are given by

$$II_2 = \frac{2}{\gamma^4} \mathrm{Im} \sum_{k=1}^{6} \eta_k N_k ,$$

with

$$\left\{ \begin{aligned}
N_1 &= \frac{\xi\alpha_3}{\nu_2^2}\left[\frac{4\nu_3\nu_4}{\nu_2^2}(11, 3, 5-7, 9) + \alpha_1(1, 5-7, 3, 5+7)\right] , \\
N_2 &= \frac{\xi\alpha_3}{\nu_2^2}\left[\frac{4\nu_3\nu_4}{\nu_2^2}(4, 12, 10, 6-8) + \alpha_1(6-8, 2, 6+8, 4)\right] , \\
N_3 &= \frac{\xi\alpha_3}{\nu_2^2}\left[\frac{4\nu_3\nu_4}{\nu_2^2}(3, 12, 9, 6-8) + \alpha_1(6-8, 1, 6+8, 3)\right] , \\
N_4 &= \frac{\xi\alpha_3}{\nu_2^2}\left[\frac{4\nu_3\nu_4}{\nu_2^2}(4, 11, 10, 5-7) + \alpha_1(5-7, 2, 5+7, 4)\right] , \\
N_5 &= f_1 f_2^*(\alpha_1^2\alpha_3 + \nu_3) + f_3 f_4^*(\alpha_2 + \nu_3) - \frac{4\nu_3^2\alpha_3}{\nu_2^2}\left(1 - \frac{4\nu_4^2}{\nu_2^2}\right) f_9 f_{10}^* - \\
&\quad - \frac{4\nu_3\nu_4\alpha_1\alpha_3}{\nu_2^2}(2, 9, 10, 1) \equiv \{1, 2, 3, 4, 9, 10\} - \frac{4\nu_3\nu_4\alpha_1\alpha_3}{\nu_2^2}(2, 9, 10, 1) , \\
N_6 &= \frac{1}{\nu_2^2}\{6+8, 5+7, 6-8, 5-7, 12, 11\} - \\
&\quad - \frac{4\nu_3\nu_4\alpha_1\alpha_3}{\nu_2^4}(5+7, 12, 11, 6+8) .
\end{aligned} \right. \tag{3.14}$$

$(h, k, l, m) \equiv f_h^* f_k + f_l^* f_m$;

$$
(3.15)\quad \left\{
\begin{aligned}
II_3 = \frac{1}{r^2}\frac{1}{q^2}\frac{2}{(4\nu_4^2-\nu_4^2)}\Big\{ & f_1\phi[\![\sigma_1\eta_3 + [\sigma_2\sigma_3 - 4\alpha_1^2\alpha_3\,(\nu_4/\nu_2)\,(\nu_2+\nu_3)]\eta_5]\!] + \\
& + f_2[\![\phi[\sigma_1\eta_2 - \sigma_2\eta_5] + F_2(q^2)\mu\eta_5 y_1]\!] + \\
& + f_3\phi[\![\sigma_4\eta_3 + [\sigma_3\sigma_5 - 4\alpha_2\,(\nu_4/\nu_2)\,(\nu_2+\nu_3)\eta_5]]\!] + \\
& + f_4[\![\phi[\sigma_4\eta_2 - \sigma_5\eta_5] + F_2(q^2)\mu\eta_5 y_2]\!] + \\
& + f_5[\![\phi\alpha_3[-\alpha_1\eta_6\,(\sigma_7 + 4\alpha_2/\nu_2) + \eta_1\sigma_8 - \eta_4\sigma_{14}] - F_2(q^2)\,\mu\sigma_6\eta_1]\!] + \\
& + f_6[\![F_2(q^2)\mu\sigma_6\eta_3 - \phi\alpha_3[\eta_3\sigma_8 + \eta_2\sigma_{14}]]\!] + \\
& + f_7\sigma_{11}[\![-\xi F_2(q^2)\mu\eta_1 + \phi\alpha_3[\alpha_1\eta_6 + \xi(\eta_1 - \sigma_3\eta_4)]]\!] + \\
& + f_8\sigma_{11}[\![\xi F_2(q^2)\mu\eta_3 - \phi\alpha_3\xi[\eta_3 + \sigma_3\eta_2]]\!] + \\
& + f_9\phi[\![\sigma_3\sigma_9 - (4(\nu_2+\nu_3)/\nu_2^2)\,Z_5]\eta_5 - \sigma_{13}\eta_3]\!] + \\
& + f_{10}[\![F_2(q^2)\mu y_3\eta_5 - \phi[\sigma_9\eta_5 + \sigma_{13}\eta_2]]\!] + \\
& + f_{11}[\![F_2(q^2)\mu\sigma_{10}\eta_1 + \phi[\eta_4\sigma_{12} - (4\alpha_3/\nu_2^2)\,Z_6\eta_6 - \sigma_{13}\eta_1]]\!] + \\
& \qquad + f_{12}[\![-F_2(q^2)\mu\sigma_{10}\eta_3 + \phi[\eta_2\sigma_{12} + \sigma_{13}\eta_3]]\!]\Big\},
\end{aligned}
\right.
$$

with

$$
(3.16)\quad \left\{
\begin{aligned}
\eta_1 &= \frac{s\cdot p_4}{M}, \\
\eta_2 &= \frac{\nu_2^2}{M}\left\{\left[1 - \frac{\nu_1}{\nu_2} - \frac{2\nu_1\nu_3}{\nu_2^2}\right](s\cdot p_4) + \frac{2\nu_1}{\nu_2^2}(\nu_2+\nu_3)\,s\cdot r\right\}, \\
\eta_3 &= -\frac{1}{M}\{2s\cdot r(\nu_2+\nu_3)(\nu_2+\nu_3-1) + \\
&\qquad + s\cdot p_4[\nu_1(\nu_2+\nu_3) + (1-\nu_2-\nu_3)(2\nu_3+\nu_2)]\}, \\
\eta_4 &= \frac{1}{M}\{-2(\nu_2+\nu_3)s\cdot r + (2\nu_3+\nu_2-\nu_1)s\cdot p_4\}, \\
\eta_5 &= \frac{2s\cdot D}{M^3}, \\
\eta_6 &= -\frac{2}{M^3}(\nu_2+\nu_3)s\cdot D; \\
\varphi &\equiv F_1(q^2) + \mu F_2(q^2);
\end{aligned}
\right.
$$

ξ and σ_i $(i = 1, \ldots, 14)$ are defined in the Appendix. II_2 and II_3 result respectively from the VPC amplitude and its interference with the BH one. In the numerator of (3.13) the pure BH term vanishes identically.

From the knowledge of R the ratio

$$\frac{\mathrm{d}\sigma(+s)}{\mathrm{d}\sigma(-s)} = \frac{1+R}{1-R}, \tag{3.17}$$

can be found, which is a more convenient quantity to be measured.

In the laboratory frame and in coincidence measurements R is given by

$$R = \left. \frac{\frac{\alpha^3}{2\pi^2}\frac{\boldsymbol{p}_3^2}{E_3}\frac{M}{k_0}\frac{|\boldsymbol{p}_4|}{|\boldsymbol{p}_1|}\frac{1}{(|\boldsymbol{p}_3|/E_3)-\hat{p}_3\cdot\hat{k}}\{II_2+II_3\}}{\mathrm{d}^5\sigma_{\mathrm{unpol}}/\mathrm{d}\Omega_3\mathrm{d}\Omega_4\mathrm{d}E_4}\right|_{\mathrm{lab}}, \tag{3.18}$$

where

$$\frac{\mathrm{d}^5\sigma_{\mathrm{unpol}}}{\mathrm{d}\Omega_3\mathrm{d}\Omega_4\mathrm{d}E_4}$$

has been defined in (3.10).

3·3. *Polarization of the recoil proton.* – In the previous Subsection we wrote down the expression of R, (eq. (3.12)), when the initial proton (target) is polarized and the polarizations of the final particles are not observed. We consider now the case of unpolarized targets and the recoil-proton polarization observed.

Likewise we define the quantity

$$R' = \frac{\mathrm{d}\sigma(+s)-\mathrm{d}\sigma(-s)}{\mathrm{d}\sigma(+s)+\mathrm{d}\sigma(-s)}, \tag{3.19}$$

where now the spin s is referred to the final proton.

R' is obtained from R by redefining the quantites η_i $(i=1,\ldots,6)$, appearing in (3.14) and (3.15) as follows:

$$\left\{\begin{aligned}
\eta_1 &= -\frac{s\cdot p_2}{M},\\
\eta_2 &= \frac{\nu_2^2}{M}\left\{\left[1+\frac{\nu_1}{\nu_2}+\frac{2\nu_1\nu_3}{\nu_2^2}\right]s\cdot p_2+\frac{2\nu_1}{\nu_2^2}(\nu_2+\nu_3)s\cdot r\right\},\\
\eta_3 &= -\frac{1}{M}\{2s\cdot r(\nu_2+\nu_3)(\nu_2+\nu_3-1)-\\
&\qquad -s\cdot p_2[(1-\nu_2-\nu_3)(2\nu_3+\nu_2)-\nu_1(\nu_2+\nu_3)]\},\\
\eta_4 &= \frac{2}{M}(\nu_2+\nu_3)s\cdot r+\frac{1}{M}(2\nu_3+\nu_2+\nu_1)s\cdot p_2,\\
\eta_5 &= \frac{2}{M^3}s\cdot D,\\
\eta_6 &= \frac{2}{M^3}(\nu_2+\nu_3)s\cdot D,
\end{aligned}\right. \tag{3.20}$$

and all the rest unchanged.

4. – Virtual-proton Compton contribution to the WAB.

In Sect. **2** the VPC amplitude $M_{\mu\nu}$ has been written in terms of the twelve amplitudes $f_i (i = 1, ..., 12)$. We now proceed to find their explicit expressions. To achieve this we approximate the blob of Fig. 1 *c*) by the contributions of a single virtual proton and a 3-3 resonance. This approximation limits our predictions to the experimental configuration in which only these states are relevant. We dismiss also π^0- and η^0-exchange contributions since it is known that they are almost negligible at and below the first resonance ([5,8]).

4·1. *Single-nucleon intermediate state.* – The contribution of the single-nucleon intermediate state to the $f_i^{'s}$ may be found by using unitarity in the manner described by HEARN and LEADER but this procedure does not guarantee the correct low-energy limit ([9]).

Instead we appeal to the low-energy Compton-scattering theorem ([10]) which states that the low-energy limit is correctly given by the lowest-order perturbation theory, if anomalous Pauli moments are included. Accordingly the single-nucleon contribution is given by

$$(4.1) \qquad M^B_{\mu\nu} = \left(\gamma_\nu + \frac{\mu}{2M}\gamma_\nu \tilde{k}\right)\frac{\tilde{p}_2 + \tilde{r} + M}{(p_2 + r)^2 - M^2}\cdot \cdot\left[F_1(r^2)\gamma_\mu + \frac{\mu}{4M}F_2(r^2)(\tilde{r}\gamma_\mu - \gamma_\mu\tilde{r})\right] + \text{crossed term}\,.$$

Now taking into account that A, B, C and D form an orthogonal basis and that $M_{\mu\nu}$ operates between two free proton Dirac spinors, and using the identity $\tilde{D} = i\gamma_5 \tilde{A}\tilde{B}\tilde{C}$, we find that

$$(4.2) \qquad \begin{cases} f_1^B = \dfrac{2\nu_2 F_1(r^2)}{\nu_1^2 - \nu_2^2} - \dfrac{2\nu_3 \mu F_2(r^2)}{\nu_2}\,, \\ f_2^B = \dfrac{\nu_1 F_1(r^2)}{\nu_1^2 - \nu_2^2} + \dfrac{2\nu_1\nu_3\big(F_1(r^2) + \mu F_2(r^2)\big)}{\nu_2(\nu_1^2 - \nu_2^2)}\,, \\ f_3^B = \mu[F_1(r^2) + (1+\mu)F_2(r^2)]\,, \\ f_4^B = -\dfrac{\nu_1}{\nu_1^2 - \nu_2^2}(1+\mu)[F_1(r^2) - \mu F_2(r^2)]\,, \end{cases}$$

([8]) A. P. CONTOGOURIS and A. VERGANELAKIS: *Phys. Rev.*, **6**, 103 (1963).

([9]) A. C. HEARN and E. LEADER: *Phys. Rev.*, **126**, 789 (1962).

([10]) F. E. LOW: *Phys. Rev.*, **96**, 1428 (1954); M. GELL-MANN and M. L. GOLDBERGER: *Phys. Rev.*, **96**, 1433 (1954).

$$
\left\{
\begin{aligned}
f_5^B &= -\frac{\mu}{2}[F_2(r^2)-F_1(r^2)]\nu_2\frac{(\nu_1^2-\nu_2^2)(\nu_2+\nu_3)+\nu_2^2}{(\nu_2+\nu_3)(\nu_1^2-\nu_2^2)}\,,\\
f_6^B &= \nu_2\frac{2F_1(r^2)+\mu[F_1(r^2)+F_2(r^2)]}{2(\nu_1^2-\nu_2^2)}+\\
&\qquad +\frac{\nu_2\nu_3\mu[F_2(r^2)-F_1(r^2)]}{2(\nu_1^2-\nu_2^2)(\nu_2+\nu_3)}-\frac{1}{2}\mu^2F_2(r^2)\,,\\
f_7^B &= \frac{\nu_2^3[2F_1(r^2)+\mu(F_1(r^2)+F_2(r^2))]}{2(\nu_2+\nu_3)(\nu_1^2-\nu_2^2)}-\mu^2F_2(r^2)\frac{\nu_2\nu_3}{2(\nu_2+\nu_3)}-\frac{\mu}{2}\nu_2\cdot\\
&\qquad \cdot[F_1(r^2)+F_2(r^2)+\mu F_2(r^2)]\,,\\
f_8^B &= -\frac{\mu^2}{2}F_2(r^2)\frac{\nu_3}{\nu_2+\nu_3}+\frac{\nu_2^2}{2(\nu_1^2-\nu_2^2)(\nu_2+\nu_3)}\cdot\\
&\qquad \cdot[2F_1(r^2)+\mu(F_1(r^2)+F_2(r^2))]-\frac{\nu_2[F_1(r^2)+\mu F_2(r^2)]}{\nu_1^2-\nu_2^2}\,,\\
f_9^B &= -\mu F_2(r^2)\nu_1\left(\frac{1}{2}+\frac{\nu_2}{\nu_1^2-\nu_2^2}+\frac{\nu_3}{\nu_2}\right),\\
f_{10}^B &= (F_1(r^2)+\mu F_2(r^2))\left[\frac{\nu_2+\nu_3}{\nu_2}+\frac{\nu_2}{\nu_1^2-\nu_2^2}\right]-\frac{\nu_1^2\mu F_2(r^2)}{2(\nu_1^2-\nu_2^2)}\,,\\
f_{11}^B &= -\mu(1+\mu)F_2(r^2)\frac{\nu_1\nu_2}{2}\left[1+\frac{\nu_2^2}{(\nu_2+\nu_3)(\nu_1^2-\nu_2^2)}\right],\\
f_{12}^B &= -\mu(1+\mu)F_2(r^2)\frac{\nu_1\nu_2^2}{2(\nu_2+\nu_3)(\nu_1^2-\nu_2^2)}-\mu^2F_2(r^2)\frac{\nu_1}{2}\,.
\end{aligned}
\right. \tag{4.2}
$$

Apart from f_8^B, these results agree with those of ref. [5].

4·2. *Meson-nucleon intermediate state.* – We now have to find the contributions of the meson-nucleon intermediate states. To face this problem the usual analysis using dispersion techniques is not suitable because it leads to excessively complicated calculations. Instead we use an isobaric model for the 3-3 resonance. This resonance can be excited electromagnetically by the magnetic dipole $M1$, transverse electric-quadrupole $E2$ and scalar-quadrupole $Q2$ transitions. The first alone is well known to give a fairly adequate fit to scattering data and so we have neglected the $E2$ and $Q2$ excitations. The magnetic-dipole isobaric formation can be described by making use of the well-known spin-$\frac{3}{2}$ partial-wave amplitude in the so-called nonrelativistic form, and by transforming it into a covariant analytic amplitude, as has been done in ref. [11]. However, since up to now we have used the familiar Dirac 4-spinor formalism, in order to maintain uniformity of our work, we shall

---

[11] A. VERGANELAKIS and D. ZWANZIGER: *Nuovo Cimento*, **39**, 613 (1965).

employ the Rarita-Schwinger spin-$\frac{3}{2}$ propagator and vertex function. As interaction for the $\gamma p \mathcal{N}^*$ vertex we choose [12]

$$H = \frac{eg}{\Delta} \bar{\psi}_\nu(x) \gamma_5 \gamma_\mu \phi(x) F_{\mu\nu} + \text{h.c.}, \tag{4.3}$$

where $\phi(x)$ is the proton field, $F_{\mu\nu}$ is the electromagnetic-field tensor and $\psi_\nu(x)$ is the spin-$\frac{3}{2}$ field of Rarita and Schwinger; and as spin-$\frac{3}{2}$ propagator

$$S_{\mu\nu}(p) = \frac{\tilde{p} + \Delta}{p^2 - \Delta^2 + i\Gamma} \left\{ g_{\mu\nu} - \frac{\gamma_\mu \gamma_\nu}{3} - \frac{1}{3\Delta}(\gamma_\mu p_\nu - p_\mu \gamma_\nu) - \frac{2}{3\Delta^2} p_\mu p_\nu \right\}, \tag{4.4}$$

where Δ and p are the mass and the four-momentum of the isobar respectively and g is a dimensionless quantity, the numerical value of which must be obtained from experiment. Γ provides the finite width of the 3-3 resonance; it is chosen such that the half-width at half-maximum $\Gamma/\Delta = (0.125 \pm 0.015)$ GeV. In the case that the photon is off the mass shell g is replaced by $gG(r^2)$ with $G(0) = 1$, where $G(r^2)$ plays the role of the form factor for the $\gamma \mathcal{N} \mathcal{N}^*$ vertex. The choice of this propagator avoids the presence of an undesirable pole in the crossed diagram but it has the limitation that outside the resonance region it no longer represents a pure angular-momentum $\frac{3}{2}$ propagator.

In analogy with the equation (4.1) we have now for the amplitude $M^{33}_{\mu\nu}$

$$M^{33}_{\mu\nu} = \left(\frac{g}{\Delta}\right)^2 G(r^2) \{(g_{\nu\varrho} k_\lambda - k_\varrho g_{\nu\lambda}) \gamma_5 \gamma_\lambda S_{\varrho\sigma}(p_4 + k) \gamma_5 \gamma_\eta (g_{\mu\sigma} r_\eta - g_{\mu\eta} r_\sigma)\} + \\ + \text{crossed term}. \tag{4.5}$$

By using the same technique as in the single-nucleon case we obtain

$$\left\{ \begin{aligned} f_1^{33} &= T(s) \left\{ \frac{M^2}{\Delta^2}(\nu_1 - \nu_2) \left[\frac{4}{3} \left(1 - \frac{\nu_1 \nu_3}{\nu_2} \right) + (\nu_1 - \nu_2) \left(2 - \frac{4}{3} \frac{\Delta}{M} \right) \right] + \right. \\ &\qquad \left. + \left[\frac{2}{3} \frac{\Delta}{M} (\nu_1 + 2\nu_2) - 2\nu_1 \right] \right\}, \\ f_2^{33} &= T(s) \left\{ \frac{4}{3} \frac{M^2}{\Delta^2} [(\nu_2 - \nu_1 - 1)[1 + (\nu_1 - \nu_2)(\nu_2 + \nu_3)/\nu_2] + \right. \\ &\qquad + \tfrac{1}{2}(\nu_1 - \nu_2)(2\nu_3 + \nu_1 - \nu_2) + \nu_1 \nu_3 / \nu_2 + (\Delta/M)(\nu_3 + \nu_1 - \nu_2)] + \\ &\qquad \left. + \frac{2}{3} \left[3 + 2\nu_3 - \frac{(\nu_2 + 2\nu_3)(\nu_1 + 2\nu_2)}{\nu_2} - \frac{\Delta}{M} \right] \right\}, \\ f_3^{33} &= \frac{2}{3} T(s) \left\{ \frac{M^2}{\Delta^2}(\nu_1 - \nu_2) \left[(2\nu_3 + \nu_1 - \nu_2) + \frac{2\Delta}{M}(\nu_2 - \nu_1) \right] + \right. \\ &\qquad \left. + \left(1 + \frac{\Delta}{M} \right)(\nu_1 + 2\nu_2) \right\}, \end{aligned} \right. \tag{4.6}$$

[12] M. GOURDIN and PH. SALIN: *Nuovo Cimento*, **27**, 309 (1963).

$$
\left\{
\begin{aligned}
f_4^{33} &= \frac{2}{3}\,T(s)\left\{\frac{M^2}{\Delta^2}(\nu_1-\nu_2)\left[2\,\frac{\Delta}{M}+(2\nu_3+\nu_1-\nu_2)+2\,\frac{\Delta}{M}\,\frac{\nu_3}{\nu_1-\nu_2}\right]+\right.\\
&\qquad\left.+(2\nu_3+\nu_1+2\nu_2)-\left(1+\frac{\Delta}{M}\right)\right\},\\
f_5^{33} &= \frac{4}{3}\,T(s)\,\frac{M^2}{\Delta^2}\,\nu_3\left[\frac{\nu_2^2}{\nu_2+\nu_3}+(\nu_1^2-\nu_2^2)\right],\\
f_6^{33} &= \frac{4}{3}\,T(s)\left\{\frac{M^2}{\Delta^2}\left[(\nu_1-\nu_2)(1+\nu_1-\nu_2)+\frac{\nu_2\nu_3}{\nu_2+\nu_3}\right]-(\nu_2+2\nu_1)\right\},\\
f_7^{33} &= -\frac{4}{3}\,T(s)\left\{\frac{\nu_2^2}{\nu_2+\nu_3}\left[\!\left[(M^2/\Delta^2)[\nu_3(1+2\Delta/M)+\right.\right.\right.\\
&\qquad\left.\left.\left.+(\nu_1-\nu_2)(1+2\nu_3+\nu_1-\nu_2)]+(2\nu_3+5\nu_2-2\nu_1)\right]\!\right]+\\
&\qquad+\frac{M^2}{\Delta^2}(\nu_1-\nu_2)^2\left[\nu_2\left(1-\frac{2\Delta}{M}\right)-\nu_3\right]+\nu_2\left(1+\frac{\Delta}{M}\right)(\nu_1-4\nu_2)\right\},\\
f_8^{33} &= \frac{4}{3}\,T(s)\,\frac{\nu_3}{\nu_2+\nu_3}\cdot\\
&\qquad\cdot\left\{\frac{M^2}{\Delta^2}\left[(\nu_1-\nu_2)(1+\nu_1-3\nu_2)-\nu_2\left(1+\frac{2\Delta}{M}\right)\right]+(3\nu_2-2\nu_1)\right\},\\
f_9^{33} &= \frac{2}{3}\,T(s)(\nu_1-\nu_2)\left\{\frac{M^2}{\Delta^2}(\nu_1-\nu_2)\left[1+\nu_1\left(1-\frac{\nu_3}{\nu_2}\right)-(\nu_2+\nu_3)-\frac{\Delta}{M}\cdot\right.\right.\\
&\qquad\left.\left.\cdot(\nu_1+2\nu_2)\right]-(\nu_2+2\nu_1)+\left(1+\frac{\Delta}{M}\right)\frac{\nu_1+\nu_2}{2}\right\},\\
f_{10}^{33} &= \frac{2}{3}\,T(s)\left\{\frac{M^2}{\Delta^2}\left[\!\left[(\nu_1-\nu_2)[(\nu_3-1)-2(\nu_1-\nu_2)-(1+\nu_3/\nu_2)(\nu_1-\nu_2)^2]+\right.\right.\right.\\
&\qquad\left.\left.\left.+(\Delta/M)[\nu_2+(\nu_1-\nu_2)(\nu_1+\nu_2+\nu_3)]\right]\!\right]+(\nu_1-\nu_2)\cdot\right.\\
&\qquad\left.\cdot\left[2-\nu_1-2\nu_2-\nu_3\left(\frac{\nu_1}{\nu_2}-2\right)\right]-\frac{1}{2}\,\nu_1\left(1+\frac{\Delta}{M}\right)\right\},\\
f_{11}^{33} &= -\,T(s)\left(\frac{\nu_2^2}{\nu_2+\nu_3}+\nu_1^2-\nu_2^2\right)\cdot\\
&\qquad\cdot\left\{\frac{2M^2}{3\Delta^2}(\nu_1-\nu_2)\left(-\frac{\Delta}{M}\,\nu_2-\nu_3\right)+\frac{1}{3}\,\nu_2\left(1+\frac{\Delta}{M}\right)\right\},\\
f_{12}^{33} &= \frac{2}{3}\,T(s)\left\{\frac{M^2}{\Delta^2}(\nu_1-\nu_2)\left[\nu_1+(\nu_1-\nu_2)^2-\frac{\nu_2}{\nu_2+\nu_3}\left(\nu_2+\frac{\Delta}{M}\,\nu_3\right)\right]-\right.\\
&\qquad\left.-\left(1+\frac{\Delta}{M}\right)\frac{\nu_2^2}{2(\nu_2+\nu_3)}-(\nu_1-\nu_2)(2\nu_1+\nu_2)\right\},
\end{aligned}
\right. \tag{4.6}
$$

where

$$T(s) = G(r^2)\left(\frac{g}{\Delta}\right)^2 \frac{M^4}{s - \Delta^2 + i\Gamma} \tag{4.7}$$

and (*) $s = M^2(1 + 2\,(\nu_1 - \nu_2))$. The crossed terms are obtained as follows:

$$f_i(\nu_1, \nu_2, \nu_3) \xrightarrow{\text{crossed}} -f_i(-\nu_1, \nu_2, \nu_3)\,, \qquad (i = 2, 4, 9, 11, 12)$$

$$f_i(\nu_1, \nu_2, \nu_3) \xrightarrow{\text{crossed}} \quad f_i(-\nu_1, \nu_2, \nu_3)\,, \qquad (i = 1, 3, 5, 6, 7, 8, 10)\,.$$

Correct p-wave threshold behaviour implies also that Γ should be multiplied by a suitable kinematical factor which we choose to be $(q/q_r)^3$, where q is the momentum of the decaying pion $\mathcal{N}^* \to \pi + \mathcal{N}$ in the rest system of the $\mathcal{N}^*$ and q_r is the value of q at the resonance ([13]).

In order to specify completely the expression of $T(s)$, the values of g^2 and $G(r^2)$ are needed. To evaluate g^2 we make use of the existing experimental data on the nonpolarized differential cross-section for Compton scattering at 90°. From the amplitudes (4.6) we take the six which contribute to the real Compton effect $f_i (i = 1, 2, 3, 4, 6, 7)$, and we consider the contribution of the 3-3 resonance at $r^2 = 0$.

We thus calculate the $(\mathrm{d}\sigma/\mathrm{d}\Omega)_{90°}$ of the real Compton scattering at the first resonance ($s = \Delta^2$). If in this expression the experimental value ([14])

$$\left(\frac{\mathrm{d}\sigma}{\mathrm{d}\Omega}\right)_{90°} = (1.6 \pm 0.2) \cdot 10^{-31}\ \mathrm{cm}^2,$$

is inserted, we obtain

$$g = 2.15 \pm 0.07\,.$$

As can be seen from eq. (4.3), the constant g has the same meaning as $C_3(0)$ of ref. ([12]), but it is differently normalized. In common normalization (used by previous authors) this value becomes $g = 0.298 \pm 0.009$; which should be compared with the values of

$$C_3(0) = 0.37\ ([12])\,, \qquad C_3(0) = 0.298\ ([15])\,, \qquad g = 0.29\ ([11])\ \text{and}\ C_3(0) = 0.3\ ([13,16])$$

(*) This s should not be confused with the s of the Sect. 3 which refers to the spin.

([13]) A. J. Dufner and Y. S. Tsai: *Phys. Rev.*, **168**, 1801 (1968).

([14]) R. F. Stiening, E. Loh and M. Deutsch: *Phys. Rev. Lett.*, **10**, 536 (1963).

([15]) J. Mathews: *Phys. Rev.*, **137**, B 444 (1965); J. D. Bjorken and J. D. Walecka: *Ann. of Phys.*, **38**, 35 (1966).

([16]) R. H. Dalitz and D. G. Sutherland: *Phys. Rev.*, **146**, 1180 (1960).

([17]) S. D. Drell: *Proc. XIII Intern. Conf. on High-Energy Physics, Berkeley, 1966.*

This agreement provides a check on our calculations. To complete the determination of the covariant isobaric contribution to the virtual Compton scattering amplitude, we have to know the explicit expression of $G(r^2)$. We have used two expressions for it. The first (choice 1) is that given by DUFNER and TSAI [13]

$$G^2(r^2) = \exp\left[-6.3\sqrt{-r^2}\right](1 + 9.0\sqrt{-r^2}) . \tag{4.8}$$

The second (choice 2) is the empirical nucleon isovector magnetic form factor [17]. This seemed reasonable since the resonance is excited by an isovector magnetic-dipole transition.

5. – Numerical calculations and results.

With the formulation described in Sect. **3** and **4** we are ready to proceed to the numerical calculations. Since no approximations have been made about the mass of the probe particle, the formalism described in the previous Sections is applicable for electrons as well as for muons. As examples we have specifically calculated first the quantity [18]

$$(\mathrm{d}^5\sigma_{\mathrm{unpol}}/\mathrm{d}\Omega_3\,\mathrm{d}\Omega_4\,\mathrm{d}E_4)_{\mathrm{lab}}$$

and second the quantities R and R' for the coincidence experiments in WAB, for two initial electron energies 0.9 and 5 GeV, in various experimental configurations.

The kinematics are fixed by the following five parameters: E_1, E_4, k_0 and u_1 and u_2, where $u_1 = -(p_1 - k)^2$ and $u_2 = -(p_3 + k)^2$ are the square of the masses of the two virtual electron states in the Bethe-Heitler graphs.

In Fig. 2*a*), 2*b*) and 2*c*) we show $\mathrm{d}^5\sigma/\mathrm{d}\Omega_3\,\mathrm{d}\Omega_4\mathrm{d}E_4|_{\mathrm{lab}}$ as a function of u_1 for fixed $E_1 = 0.90$ GeV and for various E_4, k_0 and u_2. In Fig. 3*a*), 3*b*) 3*c*) we show the same quantity but with $E_1 = 5.0$ GeV. Figures 2*a*) and 3*a*) 2*b*) and 3*b*), 2*c*) and 3*c*) correspond to the case in which the invariant mass of the intermediate proton is 1.150 GeV, 1.236 GeV and 1.350 GeV respectively. If instead of using electrons as a probe we had used muons the results shown in Fig. 2*a*), 2*b*) and 2*c*) are changed slightly while those shown in Fig. 3*a*), 3*b*) 3*c*) remain practically the same. For comparison see Table I. From these figures we can make the following observations:

---

[18] This quantity has been measured recently in two kinematical configurations by a Frascati-Napoli-Roma group at Frascati (to be published).

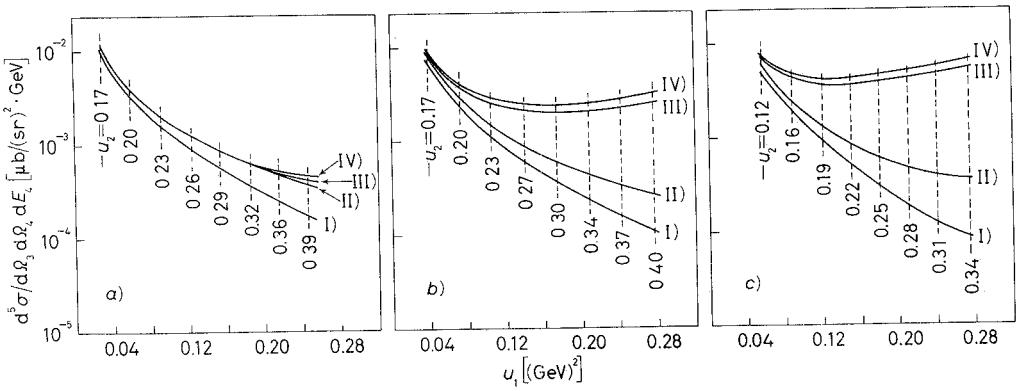

Fig. 2. – *a*) Unpolarized WAB cross-section $d^5\sigma/(d\Omega_3\, d\Omega_4\, dE_4)$ in units of 10^{-30} cm^2/GeV··(sr)^2 as a function of u_1 for $E_1 = 0.90$ GeV, $E_4 = 1.08$ GeV and $k_0 = 0.31$ GeV. Dashed lines connect the points with the same value of u_2. The curves I), II), III) and IV) are calculated respectively with: BH terms, BH+pole terms, BH+pole+3-3 resonance terms with the $\gamma\mathcal{N}\mathcal{N}^*$ form factor $G(r^2)$ given by DUFNER and TSAI, and BH+pole+3-3 resonance terms with $G(r^2)$ as the nucleon isovector magnetic form factor. *b*) The same as *a*) with $E_1 = 0.90$ GeV, $E_4 = 1.05$ GeV and $k_0 = 0.41$ GeV. *c*) The same as *a*) with $E_1 = 0.90$ GeV, $E_4 = 1.03$ GeV and $k_0 = 0.54$ GeV.

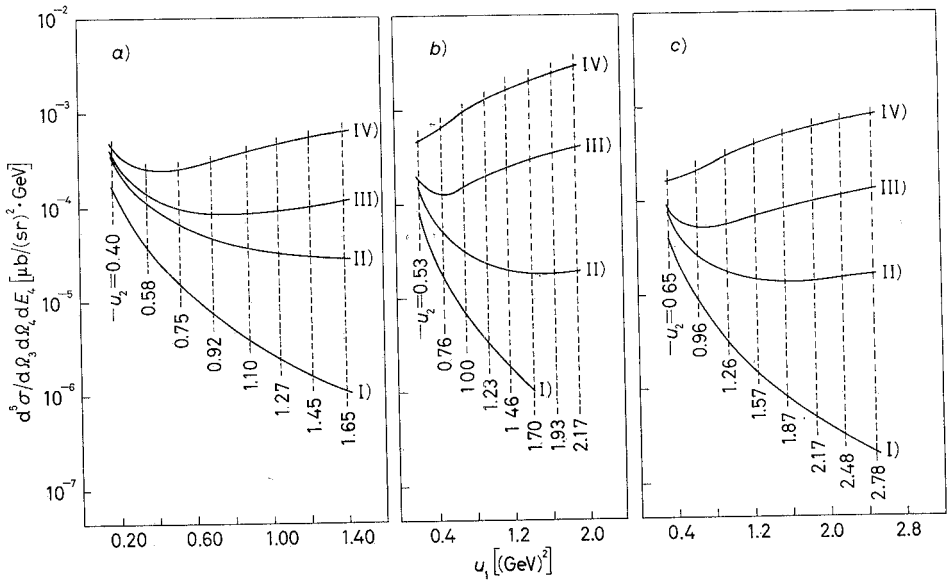

Fig. 3. – *a*) The same as Fig. 2*a*) with $E_1 = 5.0$ GeV, $E_4 = 3.04$ GeV and $k_0 = 0.35$ GeV. *b*) The same as Fig. 2*a*) with $E_1 = 5.0$ GeV, $E_4 = 2.92$ GeV and $k_0 = 0.49$ GeV. *c*) The same as Fig. 2*a*) with $E_1 = 5.0$ GeV, $E_4 = 2.84$ GeV and $k_0 = 0.7$ GeV.

a) the contributions of the VPC effect depends strongly on the kinematical configuration of the experiments and may change appreciably the results of pure QED in the critical region where the intermediate electron or muon is far off its mass shell;

TABLE I. – *Comparison between* e-p *and* μp *bremsstrahlung cross-sections*: I), II) and III) denote respectively the quantities shown in curves I), II) and III) of Fig. 2*a*).

	$E_1 = 0.9$ GeV, $E_4 = 1.05$ GeV, $k_0 = 0.413$ GeV		$E_1 = 10.0$ GeV, $E_4 = 5.54$ GeV, $k_0 = 0.358$ GeV	
	$u_1 = 0.28$ GeV^2 $u_2 = -0.40$ GeV^2	$u_1 = 0.26$ GeV^2 $u_2 = -0.41$ GeV^2	$u_1 = 2.35$ GeV^2 $u_2 = -2.38$ GeV^2	$u_1 = 2.34$ GeV^2 $u_2 = -2.39$ GeV^2
	(e^-), μb/(sr)^2 GeV	(μ^-), μb/(sr)^2 GeV	(e^-), μb/(sr)^2 GeV	(μ^-), μb/(sr)^2 GeV
I	$0.10584 \cdot 10^{-3}$	$0.10264 \cdot 10^{-3}$	$0.15188 \cdot 10^{-6}$	$0.15188 \cdot 10^{-6}$
II	$0.26262 \cdot 10^{-3}$	$0.24978 \cdot 10^{-3}$	$0.49779 \cdot 10^{-3}$	$0.49848 \cdot 10^{-3}$
III	$0.25596 \cdot 10^{-2}$	$0.23777 \cdot 10^{-2}$	0.10828	0.10825

b) at small momentum transfers to the proton the results obtained with the two form factors (choice 1) and (choice 2) used above substantially differ (see Fig. 3).

These results suggest that the exponential form factor is a more reasonable one, to describe the behaviour of the $\gamma N' N^*$ vertex form factor, in agreement with the conclusions of the analysis of the electroproduction of pions ([13]). A coincidence measurement of the WAB in the kinematical configuration of Fig. 3*b*), for example, in which the BH contribution is negligible by comparison to the VPC term, may decide for this suggestion.

It should be noticed from our calculations that the crossed graph is negligibly small at the resonance peak, while its relative magnitude is increasing as one goes outside the resonance, and there are kinematical regions where the two graphs give comparable contributions.

Let us deal now with the polarized cross-sections. To define the kinematical configurations for the quantitites R and R', in addition to the five invariants chosen for the unpolarized cross-section the orientation of the spin is needed. From now on we denote by s_2 and s_4 the spin four-directions of the target and recoil proton respectively. We have choosen our co-ordinates as

follows:

$$(5.1)\quad \begin{cases} p_1 = (E_1,\ |\boldsymbol{p}_1|,\ 0,\ 0)\,, \qquad p_2 = (M,\ 0,\ 0,\ 0)\,, \\ p_3 = (E_3,\ |\boldsymbol{p}_3|\cos\theta_e,\ |\boldsymbol{p}_3|\sin\theta_e\cos\varphi,\ |\boldsymbol{p}_3|\sin\theta_e\sin\varphi)\,, \\ p_4 = (E_4,\ |\boldsymbol{p}_4|\cos\theta_p,\ |\boldsymbol{p}_4|\sin\theta_p,\ 0)\,, \\ r = (E_1 - E_3,\ |\boldsymbol{p}_1| - |\boldsymbol{p}_3|\cos\theta_e,\ -|\boldsymbol{p}_3|\sin\theta_e\cos\varphi,\ -|\boldsymbol{p}_3|\sin\theta_e\sin\varphi) \end{cases}$$

and

$$(5.2)\quad \begin{cases} s_2^x = (0,\ 1,\ 0,\ 0)\,, \\ s_2^y = (0,\ 0,\ 1,\ 0)\,, \\ s_2^z = (0,\ 0,\ 0,\ 1)\,, \end{cases}$$

$$(5.3)\quad \begin{cases} s_4^{\parallel} = (|\boldsymbol{p}_4|,\ E_4\cos\theta_p,\ E_4\sin\theta_p,\ 0)/M\,, \\ s_4^{\perp} = (0,\ \sin\theta_p - \cos\theta_p,\ 0)\,, \\ s_4^z = (0,\ 0,\ 0,\ 1)\,, \end{cases}$$

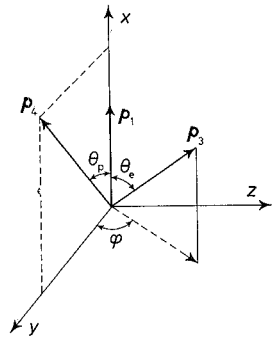

Fig. 4. – Frame of reference used to calculate the Tables II and III.

where the angles θ_e, θ_p and φ are shown in Fig. 4.

The expressions for the products occurring in the (2.16) and (3.21) can now be obtained in terms of the angles θ_e, θ_p and φ and initial and final energies. In Tables II and III we show the results.

In the above co-ordinate system ξ is given by

$$(5.4)\qquad \xi = \frac{1}{2M^3}\boldsymbol{p}_4\cdot(\boldsymbol{p}_1\times\boldsymbol{p}_3) = -\frac{|\boldsymbol{p}_1||\boldsymbol{p}_3||\boldsymbol{p}_4|\sin\theta_e\sin\theta_p\sin\varphi}{2M^3}\,.$$

TABLE II. – *The invariants $s_2\cdot p_4$, $s_2\cdot r$ and $s_2\cdot D$ expressed in terms of momentum and angles for various choices of the polarization s_2.* Quantities evaluated in the laboratory frame (Fig. 4).

$s_2^x\cdot p_4 = -\lvert\boldsymbol{p}_4\rvert\cos\theta_p$
$s_2^y\cdot p_4 = -\lvert\boldsymbol{p}_4\rvert\sin\theta_p$
$s_2^z\cdot p_4 = 0$
$s_2^x\cdot r = \lvert\boldsymbol{p}_3\rvert\cos\theta_e - \lvert\boldsymbol{p}_1\rvert$
$s_2^y\cdot r = \lvert\boldsymbol{p}_3\rvert\sin\theta_e\cos\varphi$
$s_2^z\cdot r = \lvert\boldsymbol{p}_3\rvert\sin\theta_e\sin\varphi$
$s_2^x\cdot D = -(M/2)\lvert\boldsymbol{p}_3\rvert\lvert\boldsymbol{p}_4\rvert\sin\theta_e\sin\theta_p\sin\varphi$
$s_2^y\cdot D = (M/2)\lvert\boldsymbol{p}_3\rvert\lvert\boldsymbol{p}_4\rvert\cos\theta_p\sin\theta_e\sin\varphi$
$s_2^z\cdot D = (M/2)\{\lvert\boldsymbol{p}_3\rvert\lvert\boldsymbol{p}_4\rvert(\cos\theta_e\sin\theta_p - \cos\theta_p\sin\theta_e\cos\varphi) - \lvert\boldsymbol{p}_1\rvert\lvert\boldsymbol{p}_4\rvert\sin\theta_p\}$

TABLE III. – *The same as Table II with s_2 replaced by s_4.*

$$
\begin{aligned}
s_4^{\parallel}\cdot p_2 &= |\boldsymbol{p}_4| \\
s_4^{\perp}\cdot p_2 &= 0 \\
s_4^{z}\cdot p_2 &= 0 \\
s_4^{\parallel}\cdot r &= (|\boldsymbol{p}_4|/M)(E_1-E_3)+ \\
&\quad +(E_4/M)(|\boldsymbol{p}_3|\cos\theta_e\cos\theta_p+|p_3|\sin\theta_e\sin\theta_p\cos\varphi-|\boldsymbol{p}_1|\cos\theta_p) \\
s_4^{\perp}\cdot r &= (1/M)(|\boldsymbol{p}_3|\cos\theta_e\sin\theta_p-|\boldsymbol{p}_3|\sin\theta_e\cos\theta_p\cos\varphi-|\boldsymbol{p}_1|\sin\theta_p) \\
s_4^{z}\cdot r &= |\boldsymbol{p}_3|\sin\theta_e\sin\varphi \\
s_4^{\parallel}\cdot D &= 0 \\
s_4^{\perp}\cdot D &= -(M/2)|\boldsymbol{p}_3||\boldsymbol{p}_4|\sin\theta_e\sin\varphi \\
s_4^{z}\cdot D &= (M/2)[|\boldsymbol{p}_3||\boldsymbol{p}_4|(\cos\theta_e\sin\theta_p-\cos\theta_p\sin\theta_e\cos\varphi)-|\boldsymbol{p}_1||\boldsymbol{p}_4|\sin\theta_p]
\end{aligned}
$$

Let us choose now as orientation of the spin target and of spin of the observed recoil proton the s_2^y and $s_4^{\perp}$ respectively. For these particular choices we report in Fig. 5*a*) and 5*b*) R as a function of u_1 and the rest of the kinematics is as in Fig. 2*b*) and 3*b*) respectively.

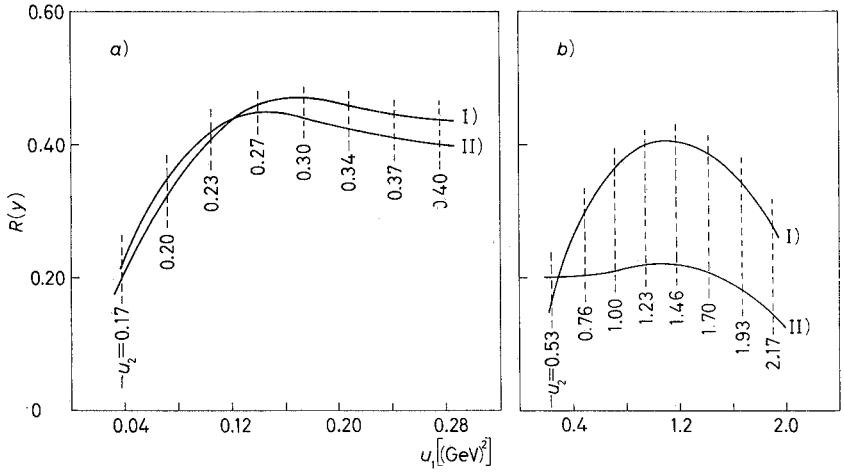

Fig. 5. – *a*) $R(y)$ defined in the text, as a function of u_1, for $E_1 = 0.90$ GeV, $E_4 = 1.05$ GeV and $k_0 = 0.41$ GeV. Dashed lines connect the points with the same value of u_2. The curves I) and II) are calculated respectively with $\gamma\mathcal{N}\mathcal{N}^*$ form factor $G(r^2)$ given by DUFNER and TSAI, and with $G(r^2)$ as the nuclear isovector magnetic form factor. *b*) The same as *a*) with $E_1 = 5.0$ GeV, $E_4 = 2.92$ GeV and $k_0 = 0.49$ GeV.

In Fig. 6*a*) and 6*b*), R' is plotted under the same circumstances as the previous Fig 5*a*) and 5*b*) respectively. As we see from these Figures, large polarization effects arise. We observe again that in the large-momentum-transfer

region, R and R' are strongly dependent on $G(r^2)$ and a measurement of R and R' can provide information about this form factor as well as about the VPC amplitude.

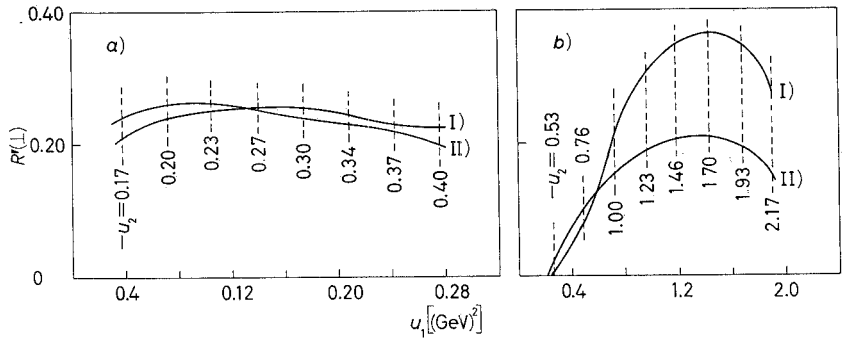

Fig. 6. – *a*) $R'(\perp)$, defined in the text, in the same kinematical configuration as Fig. 5*a*). *b*) $R'(\perp)$, defined in the text, in the same kinematical configuration as Fig. 5*b*).

In experiments in which both e^+ and e^- are available, also the interference between BH and VPC amplitude may be avoided in the numerators of R and R', provided that respectively the polarization of the target and the polarization of the recoil proton does remain the same.

Thus the WAB experiments with polarized targets, or in which the polarization of the recoil protons is measured, provide us with a good source of information about VPC amplitude.

This aim can be better achieved ([19]) in the large-angle pair-photoproduction experiments, if similar polarization measurements are made. In this case it is easy to see that in a symmetrical arrangement where charges and polarization of the final leptons are not observed, only the VPC amplitude contributes to to the numerators of R and R'. A clarification of the importance of the VPC term in this process would be valuable, because in many current theoretical interpretations of these measurements, the contribution of the nucleon isobars has been considered, in poorly justified approximations, negligibly small ([20]).

([19]) The main experimental difficulty which arises in the WAB experiments is the problem of how to discriminate the γ's of the WAB from the γ's due to the decay of the electroproduced π^0.

([20]) A. S. KRASS: *Phys. Rev.*, **138**, B 1268 (1965); S. D. DRELL: in *Proc. Intern. Symp. on Electron and Photon Interactions at High Energies, Hamburg, 1965*, vol. **1** (Berlin, 1966), p. 71; J. ASBURY, U. BECKER, W. BERTRAN, P. JOOS, M. ROHDE, A. J. S. SMITH, C. JORDAN and S. C. C. TING: *Phys. Rev. Lett.*, **19**, 869 (1967);, R. G. PARSONS and R. WEINSTEIN: *Phys. Rev. Lett.*, **20**, 1314 (1968).

6. – Discussion.

By using the covariant isobaric formalism we have been able to avoid the difficulties that arise in the present problem if dispersion relations are used. The results are of course model dependent. However, other experiments indicate that the model we have assumed should give the bulk of the VPC effect on the WAB experiments. The approximations that have been made are such that the predictions are limited to the experimental configurations in which only the single nucleon and the 3-3 resonance intermediate states are relevant: that is when the invariant mass of the intermediate proton is not far above the first resonance. According to these predictions it is legitimate to neglect the contributions of π^0 and η^0 exchange ([8]).

In our analysis we have dismissed the possible contributions from $E2$ and $Q2$. The former transition is well known from the scattering data to give a very small contribution in comparison to $M1$, while from the data of electroproduction one cannot say exactly how much the latter one contributes. Nevertheless there are well based arguments which suggest that $Q2$ cannot be large ([13]). So it is believed that the inclusion of $E2$ and $Q2$ should not change the striking features of our results. These features as we noted above are the strong dependence of the VPC effect *a*) on the kinematical configuration of the WAB experiment and *b*) on the form factor $G(r^2)$ appropriate to the vertex $\gamma\mathcal{N}\mathcal{N}^*$. From the numerical results we concluded that the $G(r^2)$ given by Dufner and Tsai seems more realistic than the empirical isovector magnetic form factors. It should be noted that this conclusion is not affected by the approximation to ignore $E2$ and $Q2$ because if for example the $Q2$ transition were significant, the form factor $G(r^2)$ would decrease still faster than that of DUFNER and TSAI ([13]).

The question of the radiative corrections detected experimentally ([21]) in the process (1.1) has not been faced in this paper and it has to be considered separately.

From the present calculations we conclude that as smaller distances are probed (as the off mass shell of the electron (muon) increases) the contributions arising from the VPC effect are relatively increasing.

* * *

We wish to thank Profs. N. CABIBBO and B. TOUSCHEK for many stimulating discussions. One of us (A.V.) is grateful to the Istituto di Fisica dell'Università di Roma and to the Laboratori del CNEN di Frascati for their support and kind hospitality. He is also indebted to Prof. B. DE TOLLIS for several interesting and helpful discussions.

([21]) H. D. SCHULZ and E. LUTZ: *Phys. Rev.*, **167**, 1280 (1968).

APPENDIX

Following ref. [5] we consider the amplitudes f_i to be functions of the three invariants ν_1, ν_2 and ν_3, defined as follows:

$$\nu_1 \equiv \frac{R\cdot K}{M^2}, \qquad \nu_2 \equiv \frac{Q^2-K^2}{2M^2}, \qquad \nu_3 \equiv \frac{Q\cdot K}{M^2} = \frac{r^2}{4M^2}.$$

We also define

$$\nu_4 \equiv \frac{(\Lambda\cdot A)}{M^2} = \frac{\lambda_1+\lambda_2}{4M^2} = \frac{(k\cdot p_1)+(k\cdot p_3)}{4M^2}$$

and

$$\nu_5 = \frac{(\Lambda\cdot R)}{M^2} = \frac{(p_1+p_3)\cdot(p_2+p_4)}{4M^2},$$

where $\Lambda = \frac{1}{2}(p_1+p_3)$.

The variables appearing in the formulae of unpolarized and polarized cross-sections are expressed in terms of the ν's as follows:

$$x = (\nu_3-\nu_2)(2\nu_3-\nu_2)/\nu_2^2,$$

$$\lambda_1 = (k\cdot p_1) = M^2(2\nu_4-\nu_2),$$

$$\lambda_2 = (k\cdot p_3) = M^2(2\nu_4+\nu_2),$$

$$r^2 = (p_1-p_3)^2 = 4M^2\nu_3,$$

$$q^2 = (p_2-p_4)^2 = 4M^2(\nu_2+\nu_3),$$

$$\mu_1 = (p_1\cdot p_2) = M^2[\nu_5+\nu_4-\nu_3-\tfrac{1}{2}(\nu_2-\nu_1)],$$

$$\mu_2 = (p_3\cdot p_4) = M^2[\nu_5-\nu_4-\nu_3-\tfrac{1}{2}(\nu_2+\nu_1)],$$

$$\mu_3 = (p_3\cdot p_2) = M^2[\nu_5+\nu_4+\nu_3+\tfrac{1}{2}(\nu_2-\nu_1)],$$

$$\mu_4 = (p_1\cdot p_4) = M^2[\nu_5-\nu_4+\nu_3+\tfrac{1}{2}(\nu_2+\nu_1)],$$

$$\alpha_1 = \nu_5+\nu_1\nu_4(2\nu_3+\nu_2)/\nu_2^2,$$

$$\alpha_2 = \frac{(\Lambda\cdot D)^2}{M^2D^2} = \left(\frac{m^2}{M^2}-\nu_3\right) + \frac{M^6}{D^2}[-(\nu_2\nu_5+\nu_1\nu_4)^2+4\nu_3(\nu_4^2-\nu_1\nu_4\nu_5)-4\nu_3\nu_4^2(\nu_2+\nu_3)],$$

$$\alpha_3 = \nu_2^2[\nu_2^2+(\nu_2+\nu_3)(\nu_1^2-\nu_2^2)]^{-1},$$

$$D^2 = M^6\nu_2^2/\alpha_3,$$

$$\xi = \tfrac{1}{2}\varepsilon_{\alpha\beta\varrho\mu}p_1^\alpha p_3^\beta p_2^\varrho p_4^\mu.$$

In addition we have

$$
\begin{aligned}
y_1 &= 2\alpha_1[\alpha_1\alpha_3(\nu_2\nu_5 - \nu_1\nu_4) + 2\nu_4^2 + \nu_2\nu_3]\,,\\
y_2 &= 2\alpha_2(\nu_2\nu_5 - \nu_1\nu_4) - \nu_2^2\alpha_1\,,\\
y_3 &= -\left(\frac{4\nu_3}{\nu_2^2}\right)\{\alpha_1\alpha_3[\nu_1\nu_2(\nu_2+\nu_3) - 2\nu_4(\nu_1\nu_4 - \nu_2\nu_5)] + \nu_4(4\nu_4^2 - \nu_2^2)\}\,,\\
Z_1 &= \nu_2\nu_4\alpha_1^2\alpha_3\,,\\
Z_2 &= \nu_2\nu_4\alpha_2\,,\\
Z_3 &= \tfrac{1}{4}\alpha_1[2\nu_2(2\alpha_2+\nu_2+\nu_3) + 4\nu_4^2 - \nu_2^2]\,,\\
Z_4 &= \tfrac{1}{4}\alpha_1[4\nu_4^2 - \nu_2^2 - 2\nu_2\nu_3]\,,\\
Z_5 &= -\alpha_1\alpha_3\nu_3(4\nu_4^2 - \nu_2^2)/\nu_2\,,\\
Z_6 &= -(\nu_3\nu_4/\nu_2)[2\alpha_2 + (4\nu_4^2 - \nu_2^2)/\nu_2]\,.
\end{aligned}
$$

The σ's are given explicitly as follows:

$$
\begin{aligned}
\sigma_1 &= \frac{\alpha_3}{\nu_2}(2\alpha_1^2\alpha_3 - \nu_2)\xi\,,\\
\sigma_2 &= 2\alpha_1\alpha_3\nu_2\left(\nu_3 + \alpha_1^2\alpha_3 + \frac{2\nu_4^2}{\nu_2}\right),\\
\sigma_3 &= \frac{\nu_1}{\nu_2}(\nu_2+\nu_3)\,,\\
\sigma_4 &= 2\,\frac{\alpha_3}{\nu_2}\left(\alpha_2+\nu_3+\frac{2\nu_4^2}{\nu_2}\right)\xi\,,\\
\sigma_5 &= \alpha_1\alpha_3\nu_2(2\alpha_2 - \nu_2)\,,\\
\sigma_6 &= \left[\sigma_7 + \frac{4}{\nu_2^2}\,\alpha_1\alpha_3(\nu_2\nu_5 - \nu_1\nu_4)\right]\xi\,,\\
\sigma_7 &= 1 + \frac{2\nu_3}{\nu_2} + \frac{4\nu_4^2}{\nu_2^2}\,,\\
\sigma_8 &= \left[\sigma_7 + \frac{4\alpha_1^2\alpha_3}{\nu_2}\right]\xi\,,\\
\sigma_9 &= 4\nu_3\nu_4\alpha_3\left[1 - \frac{4\nu_4^2}{\nu_2^2} - \frac{2\alpha_1^2\alpha_3}{\nu_2}\right],\\
\sigma_{10} &= \frac{4\nu_3\alpha_3}{\nu_2^2}\left[\frac{2\nu_4}{\nu_2}(\nu_2\nu_5 - \nu_1\nu_4) + \nu_1(\nu_2+\nu_3)\right]\xi\,,\\
\sigma_{11} &= 1 + \frac{2\nu_3}{\nu_2} - \frac{4\nu_4^2}{\nu_2^2}\,,
\end{aligned}
$$

$$\sigma_{12} = \frac{4\nu_3\alpha_3}{\nu_2^3}(\nu_2+\nu_3)\left(1-\frac{4\nu_4^2}{\nu_2^2}+\frac{2\alpha_1\alpha_3\nu_1\nu_4}{\nu_2^2}\right)\xi\,,$$

$$\sigma_{13} = \frac{8\nu_3\nu_4}{\nu_2^3}\alpha_1\alpha_3^2\xi\,,$$

$$\sigma_{14} = \sigma_3\sigma_8 - \frac{8\alpha_1\nu_4}{\nu_2^3}(\nu_2+\nu_3)\xi\,.$$

RIASSUNTO

L'effetto Compton virtuale su protone è studiato nell'approssimazione di protone virtuale singolo e risonanza 3-3 come stati intermedi. Il calcolo del secondo stato intermedio è eseguito nell'ambito del formalismo isobarico. Il contributo alla bremsstrahlung a grande angolo dovuto ai termini di effetto Compton virtuale è dato esplicitamente. Si mostra che questi contributi dipendono fortemente dalla configurazione cinematica degli esperimenti e possono cambiare sensibilmente i risultati della pura QED nella regione critica in cui l'elettrone o il muone intermedio è molto fuori del mass-shell. I risultati numerici suggeriscono che il fattore di forma esponenziale è più ragionevole per descrivere l'andamento del vertice $\gamma\mathcal{N}\mathcal{N}^*$. Inoltre si fa notare che misure di polarizzazione del protone in esperimenti di bremsstrahlung a grande angolo e produzione di coppie a grande angolo forniscono una nuova importante fonte di informazioni sul contributo dell'effetto Compton virtuale a questi processi. Le sezioni d'urto polarizzate sono calcolate esplicitamente.

Виртуальный протонный эффект Комптона и электрон (мюон-)-протонное тормозное излучение как проверка квантовой электродинамики.

Резюме (*). — Изучается виртуальный эффект Комптона в приближении единственного виртуального протона и 3-3 резонанса. Вычисление промежуточного состояния 3-3 резонанса производится в рамках изобарического формализма. Точно приводится вклад в измерения широкоуглового тормозного излучения, возникающий от членов виртуального протонного эффекта Комптона. Показывается, что эти вклады сильно зависят от кинематической конфигурации эксперимента и могут заметно изменить результаты чистой квантовой электродинамики в критической области, где промежуточный электрон или мюон находятся далеко от массовой поверхности. Численные результаты предполагают, что экспоненциальный форм-фактор является более приемлемым для описания поведения форм-фактора вершины $\gamma\mathcal{N}\mathcal{N}^*$. Кроме того, отмечается, что измерения поляризации протонов в широкоугловом тормозном излучении и экспериментах по рождению пар на большие углы представляют один из новых источников информации о вкладе виртуального протонного эффекта Комптона в эти процессы. Точно вычисляются поляризационные поперечные сечения.

(*) *Переведено редакцией.*